Dynamics and regulation of the oxidative stress response upon chemical exposure

Bischoff, L.J.M.

5

A systematic high throughput transcriptomics and phenotypic screening approach to classify the pro-oxidant mode-of-action of a large class of phenolic compounds

Luc J.M. Bischoff[1,4], Johannes P. Schimming[1,4], Wanda van der Stel[1], Marije Niemeijer[1], Sylvia Escher[3], Giulia Callegaro[1], Bas ter Braak[1], Jan P. Langenberg[2], Daan Noort[2], Bob van de Water[1]

[1]Division of Drug Discovery and Safety, Leiden Academic Centre for Drug Research, Leiden University, Leiden, The Netherlands
[2]Department of CBRN Protection, TNO Defence, Safety and Security, Rijswijk, The Netherlands
[3]Department of Chemical Safety and Toxicology, Fraunhofer Institute for Toxicology and Experimental Medicine, ITEM, Hannover, Germany.
[4]Authors contributed equally to this work

Manuscript in preparation

ABSTRACT

Oxidative stress is an important key event in many disease pathologies like cancer, Alzheimer's disease and liver diseases. Since many chemical substances can induce oxidative stress, characterizing the possibility and potency of chemicals to induce oxidative stress is of great importance for safety assessment. To evaluate the potential of oxidative stress we examined the induction of the Nrf2 response pathway for a biological read across of a diverse panel of 20 phenolic compounds including redox cyclers, non-redox cyclers, and alkylated phenols. We integrated high throughput transcriptomics using targeted RNA sequencing of primary human hepatocytes (PHH) and HepG2 and HepG2 Nrf2-GFP and Srxn1-GFP reporter cell lines. Using a panel of five pro-oxidants, including CDDO-Me, sulforaphane, *tert*-butylhydroperoxide, etacrynic acid and diethyl maleate, we identified a panel of five Nrf2 target genes that could define oxidative stress potential: *AKR1B10*, *SRXN1*, *ABCC2*, *AKR1C3* and *NQO1*. These five genes could discriminate between alkylated, redox-cyclers, and non-redox-cyclers, with strong activation of *AKR1B10* and *SRXN1* at low concentrations of redox-cyclers, and little to no activation for the alkylated phenols and non-redox-cyclers in PHH and HepG2 cells, with PHH being more vulnerable for these compounds. Subsequent high throughput confocal microscopy Nrf2 pathway activation analysis demonstrated that in particular redox-cycling phenols caused an early onset concentration-dependent activation and nuclear accumulation of the Nrf2-GFP reporter activity and subsequent induction of Srxn1-GFP. The Srxn1-GFP response and the *SRXN1* gene expression pattern were highly correlated for all phenols. In conclusion, our study demonstrates the utility to integrate both high throughput transcriptomics data from selected Nrf2 target genes with temporal response data from Nrf2 pathway GFP reporters to quantify oxidative stress induction and qualify mode-of-action of a large panel of structural similar compounds. The combination of test systems and assays might provide an innovative NAM (new approach methodology) approach for the rapid assessment of oxidative stress response to support read across-based chemical safety testing.

INTRODUCTION

Toxicity testing aims to unravel the potency of a chemical, at a certain concentration in a certain time-span to induce an adverse outcome effect. Currently, new approach methodologies (NAMs) are designed to test chemicals, including drugs, in a high throughput manner, as there is a global aim to search for alternatives to animal tests. NAMs include *in vitro* and *in chemico* assays, as well as *in silico* approaches (ECHA, 2016) and are aimed to support regulatory decisions for the use of chemicals. In particular the application of NAMs in read across has been advocated. Furthermore, the use of NAMs will improve our knowledge of the toxicokinetic and toxicodynamic properties of chemicals, making NAMs useful tools to provide input for read-across studies (Escher et al. 2019; Graepel et al. 2019; Parish et al. 2020). The rapid development and broad use of NAMs, including high throughput test systems and the use of integrated approaches e.g. combining *in vitro* and *in silico* models, has led to an increased role and understanding of stress response pathways (toxicity pathways) in modern toxicity testing (Benfenati et al. 2019; Perkins et al. 2019; Wambaugh et al. 2019). As these pathways play an important role in the response to xenobiotic exposure, cellular damage and disease, knowledge of these pathways is of great importance in the development of NAMs for the early detection of toxicity and therefore safety assessment in general. Here we addressed the question whether specific toxicity pathway testing can be applied for read across evaluation based on biological similarity. We focused here on the assessment of NAMs for the assessment of the toxicodynamics of a diverse group of phenolic compounds with a focus on the Nrf2 antioxidant stress signaling pathway named after the transcription factor nuclear factor erythroid 2-related factor 2 (Nrf2), which is the gene product of *NFE2L2*.

Under basal conditions, Nrf2 is bound in the cytoplasm to two Kelch-like ECH-associated protein 1 (Keap1) proteins (Keum and Choi 2014; Zipper and Mulcahy 2002), ubiquitinated and degraded via the ubiquitin-26S proteasomal pathway (Kobayashi et al. 2004). Upon activation by oxidative stress, caused by reactive oxygen species or electrophilic compounds (Figure 1A and 1B) (Takaya et al. 2012), degradation via the ubiquitin-26S proteasomal pathway is prevented and newly produced Nrf2 proteins are now able to translocate to the nucleus. In the nucleus, Nrf2 will bind to the antioxidant response element (ARE), which in turn will lead to the expression of a battery of antioxidant response genes including amongst others sulfiredoxin1 (Srxn1) (Copple et al. 2019; Figure 1B). Srxn1 was first discovered in yeast (Biteau et al. 2003) but is known to be present in all eukaryotes. Srxn1 plays a role in the reduction of oxidized peroxiredoxin and reversal of glutathionylation (Findlay et al. 2006; Jeong et al. 2006). Since endogenous levels of Srxn1 are relatively

low, but are strongly induced by Nrf2 activation, Srxn1 is an excellent biomarker to determine the potency and dynamics of Nrf2 activation in liver hepatocytes (Bischoff et al. 2019; Wink et al. 2018). Yet other transcriptomic biomarkers are also considered strongly indicative for Nrf2 activation (Copple et al. 2019).

A class of widely used chemical compounds, known to activate the Nrf2 pathway are phenolic compounds (phenols/quinones). In daily life, humans are exposed to phenols/quinones via diet, medicine intake, or environmental chemicals (Kyselova 2011). Despite the fact that these compounds might be beneficial due to their antioxidant properties, they are also related to hepatotoxicity (Kyselova 2011). Quinones are Michael acceptors and are able to covalently bind to cellular nucleophiles such as glutathione (GSH), resulting in depletion of GSH (Attia 2010; Bolton and Dunlap 2017). Quinones can be enzymatically reduced to hydroquinones (two electron reduction) or to semiquinones (one electron reduction) (Monks et al. 1992). Two major toxicity mechanisms are described in literature concerning quinones: ROS formation and arylation/alkylation (Xiong et al. 2014) as displayed in Figure 1C. The redox potential of a quinone is influenced by substituent effects, with addition of an electronegative substitute usually leading to a much stronger oxidant (Monks and Lau 1997). A broad overview of quinone toxicity has been published before (Bolton et al. 2000). The application of high throughput NAMs to classify the mode-of-action as well as the potency of different phenolic compounds has so far not been evaluated.

Here we used a large panel of phenols to characterize their redox-cycling-mediated oxidative stress potential. As NAMs we used high throughput transcriptomics approaches and evaluated the effects of these phenols on oxidative stress pathway activation in primary human hepatocytes as well as HepG2 hepatocarcinoma cells. Moreover, we used our established HepG2-Nrf2-GFP and HepG2-Srxn1-GFP phenotypic reporter system in combination with live cell imaging (Wink et al. 2017) to define the dynamics and potency of phenol-mediated Nrf2 pathway activation.

METHODS

Chemicals

A phenolic compound set was used which consisted of three different classes of phenolic compounds (Figure 1D): 6 hydroquinone like compounds with anticipated redox-cycling potential (redox cyclers); 12 phenolic compounds with alkyl side chain without anticipated redox-cycling potential (alkylated phenols), 2 non-alkylated and redox-cycling negative (non-redox cyclers). Chemicals were purchased from Sigma

Figure 1. Phenol toxicity mechanisms.

A) Modulation of Keap1 by phenols. **B)** Nrf2 pathway activation and downstream target activation. **C)** Radical formation of phenols. **D)** Chemical structures of the three different classes of phenolic compounds used in this study.

A)

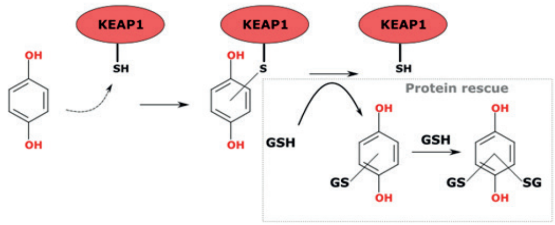

B)

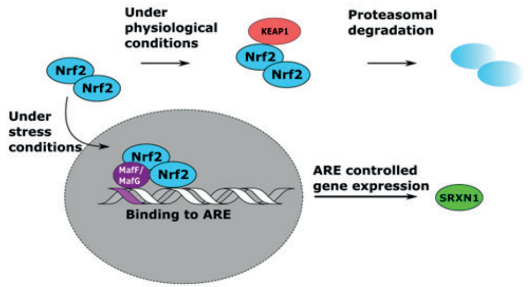

C)

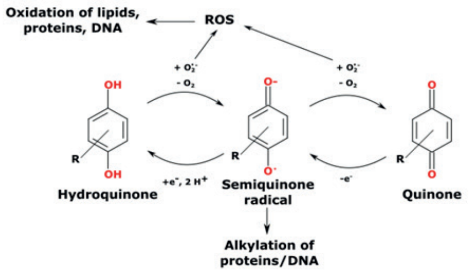

D)

Redox cyclers

Catechol Cas nr.: 120-80-9	**Hydroquinone** Cas nr.: 123-31-9	**Menadione** Cas nr.: 58-27-5
tert-Butylhydroquinone Cas nr.: 1948-33-0	**Tetramethyl-p-phenylenediamine** Cas nr.: 637-01-4	**Trimethylbenzene-1,4-diol** Cas nr.: 700-13-0

Non-redox cyclers

Phenol Cas nr.: 108-95-2	**Resorcinol** Cas nr.: 108-46-3

Alkylated phenols

2-(1,1-dimethylethyl)phenol Cas nr.: 88-18-6	**2,4-Dimethylphenol** Cas nr.: 105-67-9	**2,4-Di-tert-butylphenol** Cas nr.: 96-76-4
2,3,5-Trimethylphenol Cas nr.: 697-82-5	**2,3,6-Trimethylphenol** Cas nr.: 2416-94-6	**2,6-Dimethylphenol** Cas nr.: 576-26-1
2,6-Di-tert-butyl-4-ethylphenol Cas nr.: 4130-42-1	**2,6-Di-tert-butyl-p-cresol** Cas nr.: 128-37-0	**2,6-Di-tert-butylphenol** Cas nr.: 128-39-2
4-Methylphenol Cas nr.: 106-44-5	**4-tert-Octylphenol** Cas nr.: 140-66-9	**p-tert-Butylphenol** Cas nr.: 98-54-4

Aldrich (Amsterdam, Netherlands), or from TCI (Rotterdam, Netherlands). Upon arrival chemicals were diluted in DMSO (Sigma Aldrich (USA)) to stock concentrations of 500 mM, except for catechol, hydroquinone, resorcinol, phenol, diquat bromide monohydrate and TMPPD which were diluted in PBS to stock concentrations of 50 mM. All stocks were aliquoted and stored at -20 °C for experimental use. Concentration ranges of the compounds used for experiments were derived from literature and pilot experiments with HepG2 cells.

Cell culture

Primary human hepatocytes (PHH) and the human hepatoma cell line HepG2 were used for gene expression analysis. Cryopreserved PHH cells (LiverPool, 10 donor, #X008001 Lot: KCB, BioIVT) were thawed in OptiThaw Hepatocyte medium (Sekisui XenoTech, #K8000) and subsequently seeded at a density of 70,000 cells per well (0.32 cm^2) plating medium in INVITROGRO CP Medium (BioIVT, #Z99029) on Corning BioCoat collagen I coated 96-well plates (Corning, #08-774-5). 6 h after seeding the plating medium was exchanged with maintenance InVitroGRo Hi Medium (BioIVT, #Z99029). 24 h after seeding the PHHs were exposed to the test compounds in InVitroGRo Hi Medium.

HepG2 cells (ATCC, Wesel, Germany, clone HB8065) were grown in Dulbecco's Modified Eagle Medium (DMEM, GIBCO, #41966-029) high glucose, supplemented with 10 % (v/v) fetal bovine serum (FBS, GIBCO, #10270-106), 25 U/mL penicillin and 25 µg streptomycin (Pen Strep, GIBCO, #15070-063). For fluorescent protein reporter activity analysis we used HepG2-Srxn1-GFP and HepG2-Nrf2-GFP. These fluorescent protein reporter cell lines are bacterial artificial chromosomes (BAC)-based and developed and characterized previously (Wink et al. 2017). HepG2 cells were used for experiments until passage 20. Cells were seeded in a 96-well plate (23.000 cells/well, Greiner Bio One, #655090) for transcriptomic analysis, and exposed 72 h after plating. For GFP reporter measurement, cells were seeded in a 384-well plate (8.000 cells/well, Greiner Bio One, #781091) and exposed to the compounds 48 h after plating.

TempO-Seq assay

For transcriptome analysis, 24 h after treatment the cells were washed with PBS and lysed with 1X BioSpyder Lysis Buffer (BioSpyder, #P/N N041L). The lysate was stored in v-bottom plates on -80 °C until shipment on dry ice to BioClavis (UK) for TempO-Seq analysis. The TemO-Seq assay is a template oligonucleotide annealing and ligation assay combined with a sequencing readout for high-throughput targeted RNAseq transcriptomics (Yeakley et al. 2017). We used this technology to measure gene expression patterns after compound exposure in HepG2-WT cells and PHHs.

Therefore the cells were seeded and allowed to attach for 24 h before exposure to the test compounds. After 24h of treatment, wells were washed with 200 µL PBS and lysed with 50 µL BioSpyder 1x lysis buffer for 5 minutes at ambient temperature (20 to 24 °C). Lysate plates where sealed and immediately frozen at -80 °C. The lysate plates where shipped on dry ice to BioClavis for TempO-Seq analysis using the EU-ToxRisk S1500+ v2 gene set, an extension of the S1500+ gene set developed by the US NIEHS-National Toxicology Program. Briefly, a set of genes were identified on the basis of their diversity, co-expression and pathway coverage as found in publicly available transcriptomic data sets. Combined with the nominated genes by a Tox21 expert panel, this formed the S1500 gene set (Mav et al. 2018). Next, the gene set was used to extrapolate the whole transcriptome and genes were added to reach optimal performance resulting in the S1500+ gene set (Bushel et al. 2018). An additional group of genes was added by experts of the EU-ToxRisk consortium to meet scientific application for the project resulting in the EU-ToxRisk S1500+ v2 gene set (Daneshian et al. 2016). To cover this gene set of 3257 genes, 3561 different TempO-Seq probes were used.

Nrf2 gene set

To acquire a liver specific gene set regulated by the Nrf2 pathway, we overlapped the EU-ToxRisk S1500+ v2 gene set with the experimentally derived Nrf2 target gene list of human liver hepatocytes (Copple et al. 2019). The latter gene list is based on a siRNA knockdown (KD) screen of primary human hepatocytes with siKEAP1 and siNFE2L2 whole transcriptome analysis. All genes identified showed a significant upregulation under siKEAP1 KD and a significant downregulation under siNFE2L2 KD as compared to a scrambled siRNA control resulting in a list of 108 genes of which 36 overlap with the EU-ToxRisk S1500+ v2 gene set. The overlapping gene list is annexed in Suppl. Table 1.

Live confocal imaging

Fluorescent protein reporter activity was determined by live cell confocal imaging using a Nikon Eclipse Ti confocal microscope equipped with four lasers: 366, 408, 488 and 561 nm. A 20x dry PlanApo VC NA 0.75 with 1x zoom was used. Prior to exposure, $Hoechst_{33342}$ 100 ng/mL was added to the wells to stain nuclei and propidium iodide (PI) was added to measure cell death. Images were taken on specific time points or for a period of 24 h (1 image per hour).

Transcriptomics and imaging data analysis

The differentially expressed genes (padj <0.05) were identified by the DESeq2 method (Love et al. 2014) using the therein described R package DESeq2. The cutoff for sample exclusion was a total count of 100,000. The dose response modelling was

conducted in BMDExpress version2.2 (Phillips et al. 2018). For the identification of a dose response, BMDExpress fitted several different curves following continuous functions towards the fold change dose response of every probe. Specifically, a linear function, exponential functions of the order 2, 3, 4 and 5, polynomial functions of second degree, hill model functions and power model functions. For each probe and function type maximal 250 iterations were done and as a cutoff for the bench mark response one standard deviation above or below baseline (confidence interval of 0.95).

Microscopy images were analyzed at the single cell level using Cell Profiler and R as previously described (Schimming et al. 2019). The fraction of GFP-positive cells where calculated by counting the amount of cells with a GFP-value two times above baseline (DMSO control) level.

RESULTS

Determination of the liver specific oxidative stress response gene panel

We firstly systematically identified the relevant oxidative stress response genes that are represented in the targeted EU-ToxRisk S1500+ V2 TempO-Seq gene panel. As a first step we treated HepG2 cells with five different well known Nrf2 pathway inducing compounds: bardoxolone methyl (CDDO-Me), diethyl maleate (DEM), *tert*-butylhydroperoxide (tBHP), etacrynic acid and sulforaphane. For each of these compounds the number of significantly (padj <0.05) up- and down-regulated genes in the EU-ToxRisk S1500+ v2 gene panel was calculated after exposing HepG2 cells to different concentrations for 24 hours. We observed an increased number of differentially expressed genes with exposure to an increasing concentration of all five pro-oxidants (Figure 2A). For DEM and etacrynic acid the number of differentially expressed genes is lower after exposure to the highest concentrations, which is likely due to onset of cell death at these high concentration. Next, we investigated the effect on genes related to the Nrf2 oxidative stress response pathway. We selected a set of 36 genes that are affected by *KEAP1* and *NFE2L2* knockdown in primary human hepatocytes and are in overlap with our targeted gene panel (Copple et al. 2019). For the entire gene set we rank ordered the absolute maximum expression changes after compound exposure across all concentrations, and projected the 36 Nrf2-related genes in red (padj<0.05) (Figure 2B). We observed that two of the Nrf2 target genes, *AKR1B10* and *SRXN1*, demonstrated the strongest activation for all five compounds and were consistently the two most responsive genes of the 36-gene set. Other Nrf2 target genes did not show any apparent different pattern from other

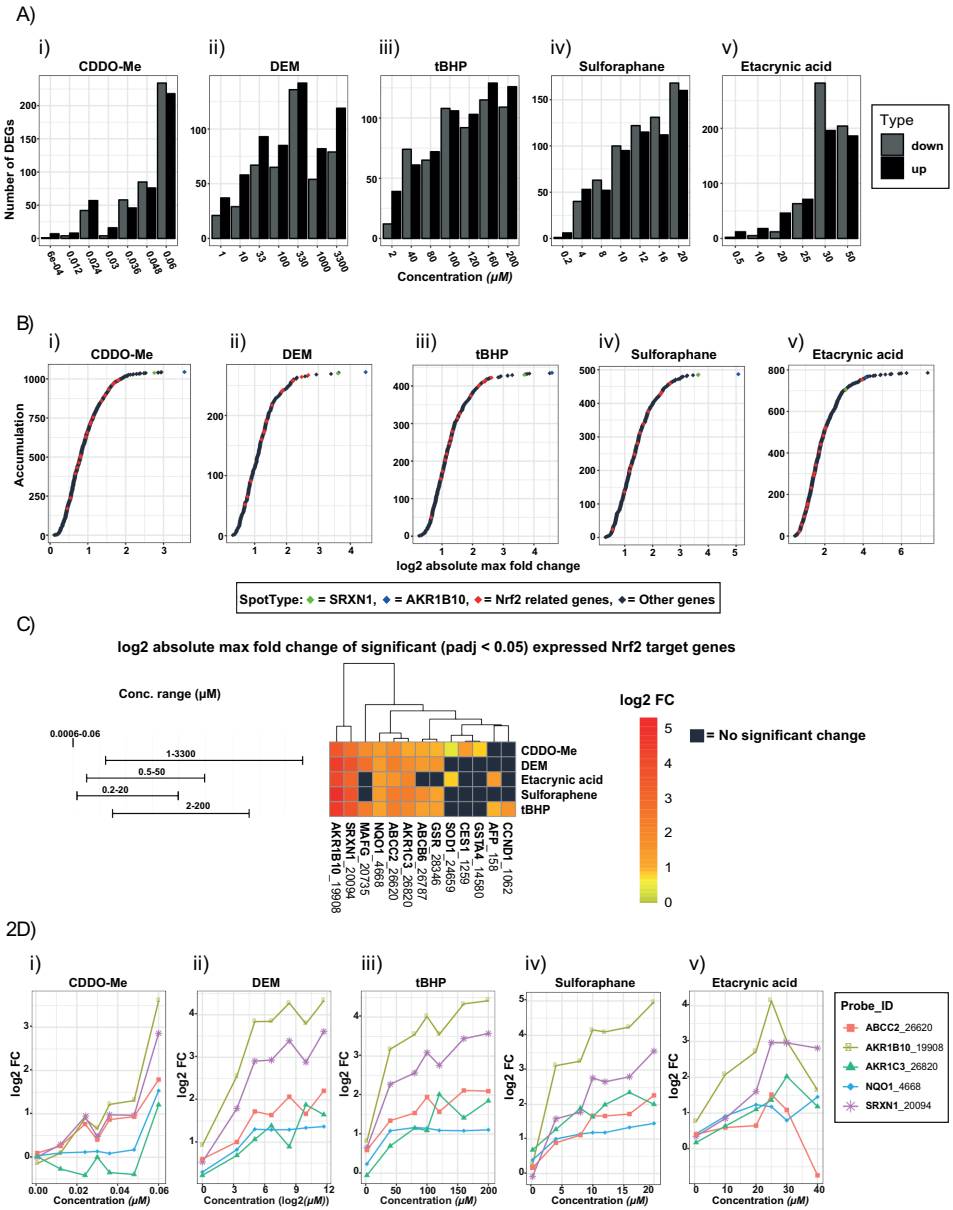

Figure 2. Gene expression response upon treatment with the selected positive controls.

A) Number of significant (padj<0.05) differently expressed genes (up/down regulated) at different compound concentrations. **B)** Accumulation plots of the significant (padj<0.05) expressed genes ranked to the log2 absolute maximal fold change. Green = SRXN1, blue is AKR1B10, red = selected Nrf2 related genes, and black = other significant expressed genes after exposure to the different positive controls. **C)** Heatmap of the maximal log2 FC of significant (padj<0.05) expressed Nrf2 related genes (gene_probe combination). Column clustering is based on Euclidean method. **D)** Dose-response (log2 FC) curves of the positive controls for the five highest significantly (padj<0.05) differentially expressed Nrf2 related genes after exposure to the different positive controls.

differentially expressed genes. It should be noted that the concentration at which the maximal fold change was reached is not taken into account as we only looked at the maximum fold change that could be reached over the entire concentration range. As a next step, we wondered which of the Nrf2 target genes were significantly (padj<0.05) differently expressed (log2 FC) after exposure to the five different pro-oxidants. We found 13 of the 36 Nrf2 target genes to be significantly differently expressed by at least one compound across the full concentration range. The highest fold changes across all five compounds were found for *AKR1B10* and *SRXN1*, followed by *ABCC2*, *AKR1C3* and *NQO1* (Figure 2C). All of these five Nrf2 target genes showed a concentration dependent induction, with *AKR1B10* and *SRXN1* being the most sensitive across the entire concentration range (Figure 2D). These data indicate that this selective panel of five Nrf2 target genes is a good representative for pro-oxidant Nrf2 activation in HepG2 cells.

Nrf2 target gene expression patterns in HepG2 cells and primary human hepatocytes after exposure to the different phenolic compounds

Next, we investigated the potency of activation of the Nrf2 pathway of the different phenolic compounds belonging to one of the three different groups: redox cyclers, non-redox cyclers, and alkylated phenols. We first focused on activation of the five selected Nrf2 target genes (Figure 3A). In general, we found higher activation of these genes after exposure to the redox cyclers, with trimethylbenzene-1,4-diol being the most potent. *SRXN1* and *AKR1B10* showed the strongest response after exposure to the redox cyclers. No response was observed for the two highest concentrations of 2-methyl-1,4-naphtoquinone due to cell death after 24 h exposure. Interestingly, also some alkylated compounds, in particular 2,4-dimethylphenol, demonstrated activation of Nrf2 target genes, albeit at higher concentrations. As expected, the two non-redox cyclers (phenol and resorcinol) showed hardly any response. Next, we compared the maximum fold change (log2 FC) of all the Nrf2 target genes (padj<0.05) and included only those genes for which at least a significantly differentially expression was observed for one compound. The redox-cycling phenols resulted in a higher response of these genes, compared to the non-redox cyclers and alkylated phenolic compounds (Figure 3B). Also other genes, including *MTLL11* and *CCND1* were activated. So far, these data only indicated a possibility to activate these Nrf2 target genes, but did not provide information on the potency. Therefore we also determined the bench mark concentration (BMC) for all compounds for the set of significantly affected Nrf2 target genes. We observed that redox-cycling phenols did activate the Nrf2-related genes at lower concentrations than alkylated phenols (Figure 3C); 2,4-dimethylphenol was the exception as the most responsive alkylated phenol. Next, we wondered whether we could classify the three classes of phenolic compounds only based the FC and BMC information of the five Nrf2

A)

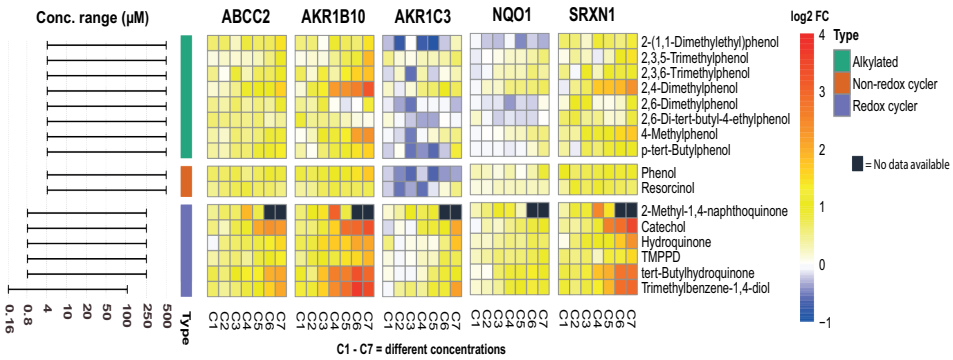
Conc. range (µM)
0.16
0.8
4
10
20
50
100
250
500
Type
ABCC2
AKR1B10
AKR1C3
NQO1
SRXN1
C1 C2 C3 C4 C5 C6 C7
2-(1,1-Dimethylethyl)phenol
2,3,5-Trimethylphenol
2,3,6-Trimethylphenol
2,4-Dimethylphenol
2,6-Dimethylphenol
2,6-Di-tert-butyl-4-ethylphenol
4-Methylphenol
p-tert-Butylphenol
Phenol
Resorcinol
2-Methyl-1,4-naphthoquinone
Catechol
Hydroquinone
TMPPD
tert-Butylhydroquinone
Trimethylbenzene-1,4-diol
log2 FC
4
3
2
1
0
−1
Type
Alkylated
Non-redox cycler
Redox cycler
= No data available
C1 - C7 = different concentrations

B)

i)

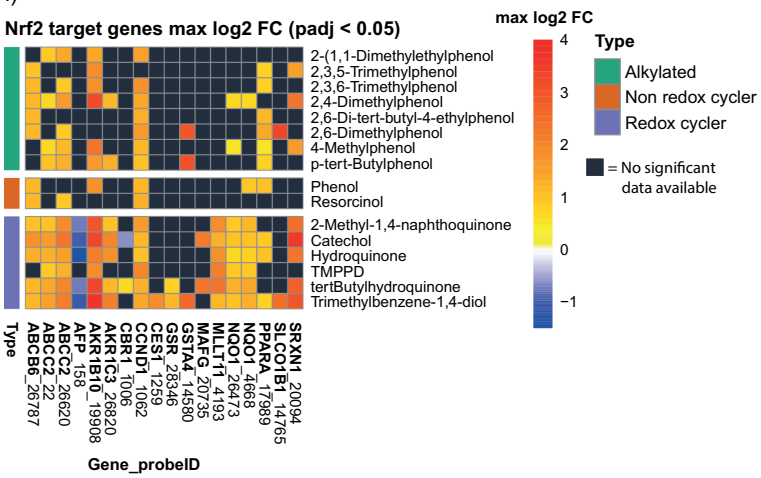
Nrf2 target genes max log2 FC (padj < 0.05)
max log2 FC
4
3
2
1
0
−1
Type
Alkylated
Non redox cycler
Redox cycler
= No significant
data available
2-(1,1-Dimethylethyl)phenol
2,3,5-Trimethylphenol
2,3,6-Trimethylphenol
2,4-Dimethylphenol
2,6-Di-tert-butyl-4-ethylphenol
2,6-Dimethylphenol
4-Methylphenol
p-tert-Butylphenol
Phenol
Resorcinol
2-Methyl-1,4-naphthoquinone
Catechol
Hydroquinone
TMPPD
tertButylhydroquinone
Trimethylbenzene-1,4-diol
Type
ABCB6_26787
ABCC2_22
ABCC2_26620
AFP_158
AKR1B10_19908
AKR1C3_26820
CBR1_1006
CCND1_1062
CES1_1259
GSR_28346
GSTA4_14580
MAFG_20735
MLLT11_4193
NQO1_4668
NQO1_26473
PPARA_17989
SLCO1B1_14765
SRXN1_20094
Gene_probeID

ii)

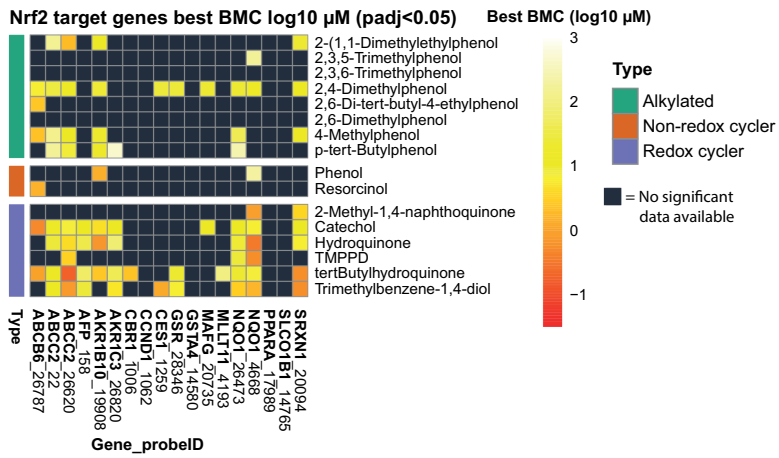
Nrf2 target genes best BMC log10 µM (padj<0.05)
Best BMC (log10 µM)
3
2
1
0
−1
Type
Alkylated
Non-redox cycler
Redox cycler
= No significant
data available
2-(1,1-Dimethylethyl)phenol
2,3,5-Trimethylphenol
2,3,6-Trimethylphenol
2,4-Dimethylphenol
2,6-Di-tert-butyl-4-ethylphenol
2,6-Dimethylphenol
4-Methylphenol
p-tert-Butylphenol
Phenol
Resorcinol
2-Methyl-1,4-naphthoquinone
Catechol
Hydroquinone
TMPPD
tertButylhydroquinone
Trimethylbenzene-1,4-diol
Type
ABCB6_26787
ABCC2_22
ABCC2_26620
AFP_158
AKR1B10_19908
AKR1C3_26820
CBR1_1006
CCND1_1062
CES1_1259
GSR_28346
GSTA4_14580
MAFG_20735
MLLT11_4193
NQO1_4668
NQO1_26473
PPARA_17989
SLCO1B1_14765
SRXN1_20094
Gene_probeID

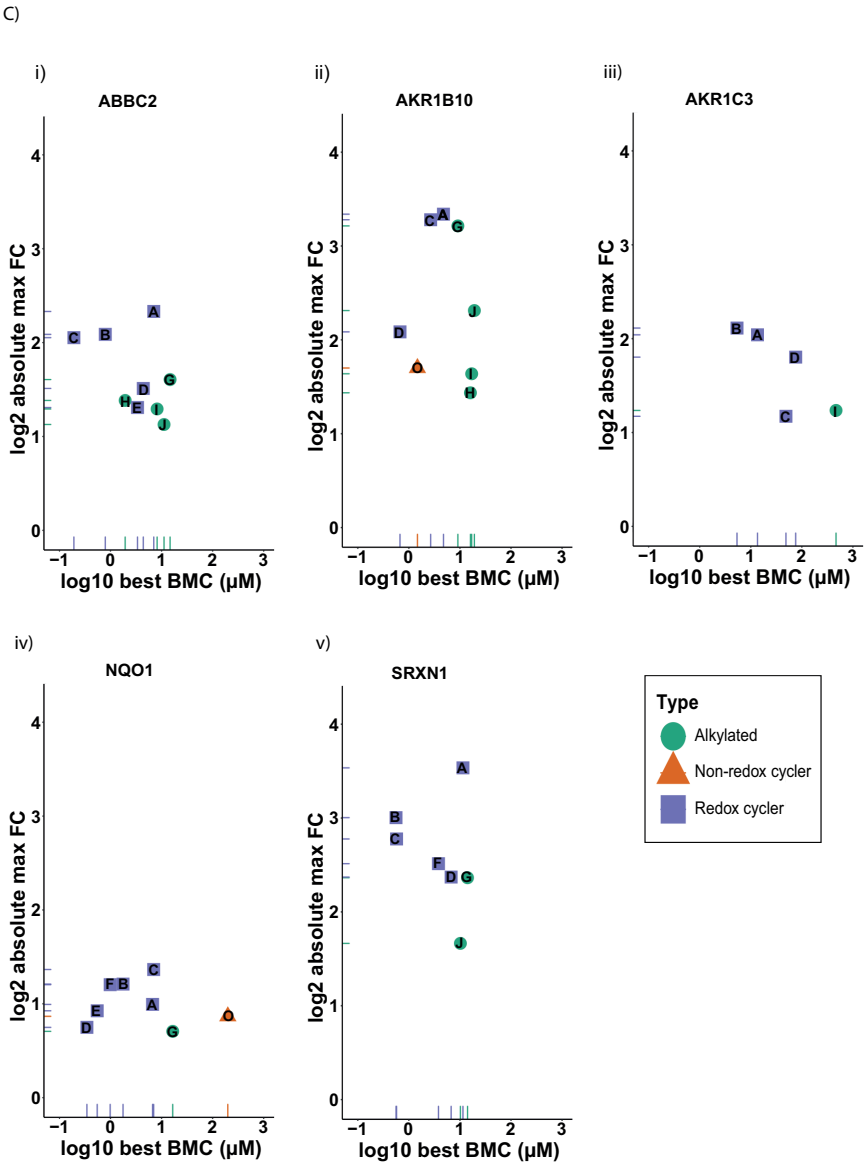

Figure 3. Nrf2 related gene expression of HepG2 cells after exposure to different phenolic compounds.

A) Heatmap showing the dose response of the five most responsive Nrf2 related genes. Note the different concentration ranges for the various phenols. **B)** i) Heatmap showing the significant (padj<0.05) max (highest positive value (upregulation) and otherwise highest negative value (down regulation)) log2 maximal fold changes of all the Nrf2 target genes across the entire concentration range. ii) Heatmap showing the significant (padj<0.05) best BMC (benchmark concentration) (log10µM) of the Nrf2 related genes **C)** Scatterplot best log10 BMC vs log2 max absolute FC for the five most response Nrf2 related genes for the three different classes of phenolic compounds. A = Catechol, B = Trimethylbenzene-1,4-diol, C = tert-Butylhydroquinone, D = Hydroquinone, E = TMPPD, F = 2-Methyl-1,4-naphthoquinone, G = 2,4-Dimethylphenol, H = 2-(1,1-Dimethylethyl)phenol, I = p-tert-Butylphenol, J = 4-Methylphenol, K = 2,3,6-Trimethylphenol, L = 2,3,5-Trimethylphenol, M = 2,6-Dimethylphenol, N = 2,6-Di-tert-butyl-4-ethylphenol, O = Phenol, P = Resorcinol.

target genes (Figure 3C). We observed the same pattern for all five genes, as redox-cycling phenols present in the upper left corner (high max absolute log2 FC and a low best log10 BMC) and alkylated compounds present in the lower right corner. The non-redox cycling phenols did not show a significant response for most of the five genes except for *AKR1B10* and *NQO1*. These data support the notion that this panel of five Nrf2 target genes provides a good basis for classifying the phenolic compounds based oxidative stress activation. Based on the responses of these five genes we were largely able to separate the active redox cycling phenols from the other phenolic compound classes.

As a next step, we wondered whether we would observe the similar Nrf2 target gene activation in primary cultured human hepatocytes (PHH) based on a pool of 10 different donors. Therefore, PHH were exposed for 24 hours to a selected set of different phenolic compounds used for the HepG2 cells; we included all redox cycling phenols, yet reduced the number of alkylated phenols and non-redox cycling phenols. Viability assays showed a high sensitivity of the PHH to redox cycling phenols with a steep concentration response (Suppl. Figure 1). Limited cytotoxicity was observed for the alkylated phenols and phenol. This indicates that PHH are more sensitive for onset of cell death by redox cycling phenols than HepG2 cells, with 2-methyl-1,4-naphtoquinone being most potent. Cytotoxicity was associated with low number of total TempO-Seq read counts; due to the cytotoxicity we could not determine the activation of Nrf2 target genes at these cytotoxic concentration. Regardless, at the non-cytotoxic concentrations we did observe activation of Nrf2 target genes, with *SRXN1* and *AKR1B10* being most prominent (Figure 4A), albeit that the maximum fold change induction was limited compared to HepG2 cells.

We extended our analysis to all the differential expressed Nrf2 target genes. Irrespective of the limitation on the dose response information due to the cytotoxicity, we determined the max log2 FC values for all other Nrf2 target genes as well as the log10 best BMC (Figure 4B). Other Nrf2 target genes also showed induction depending on phenol compound treatment, including *CBR3*, *ADHB4*, *MAFG*, *OSGIN1* and *SULT1A2*, but the overall max log2 FC values could not discriminate between redox-cycling and alkylated phenolic compounds. Similarly, the log10 best BMC did not show drastic lower BMC values for redox-cycling phenols, with the caveat that the cytotoxicity of redox cycling phenols prohibited accurate BMC calculation due to loss of full dose response information. In particular for the most cytotoxic phenol compound 2-methyl-1,4-naphtoquinone this hampered determination of realistic BMC values. Further plotting of the log10 best BMC against the max absolute log2 FC for Srnx1 showed the best separation of the redox-cyclers from the alkylated phenolic compounds. Overall, comparing the transcriptomics response of HepG2 cells with

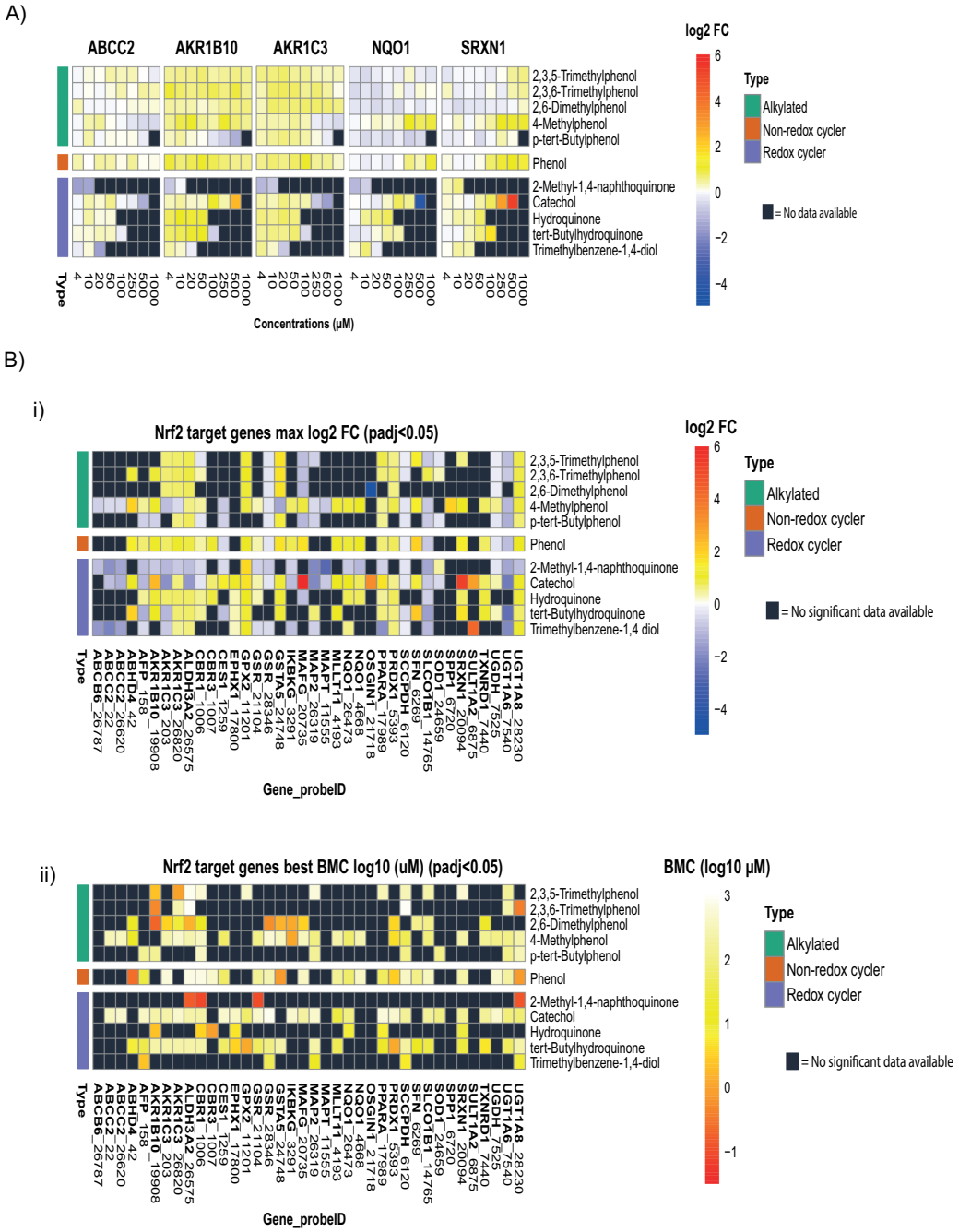

Figure 4. Nrf2 target gene expression of PHH cells after exposure to different phenolic compounds.

A) Heatmap showing the dose response of the five most responsive Nrf2 target genes. **B)** i) Heatmap showing the significant (padj<0.05) max (highest positive value (upregulation) and otherwise highest negative value (down regulation)) log2 maximal fold changes of all Nrf2 target genes that are differentially expressed at any of the treatment concentrations. ii) Heatmap showing the significant (padj<0.05)

C)

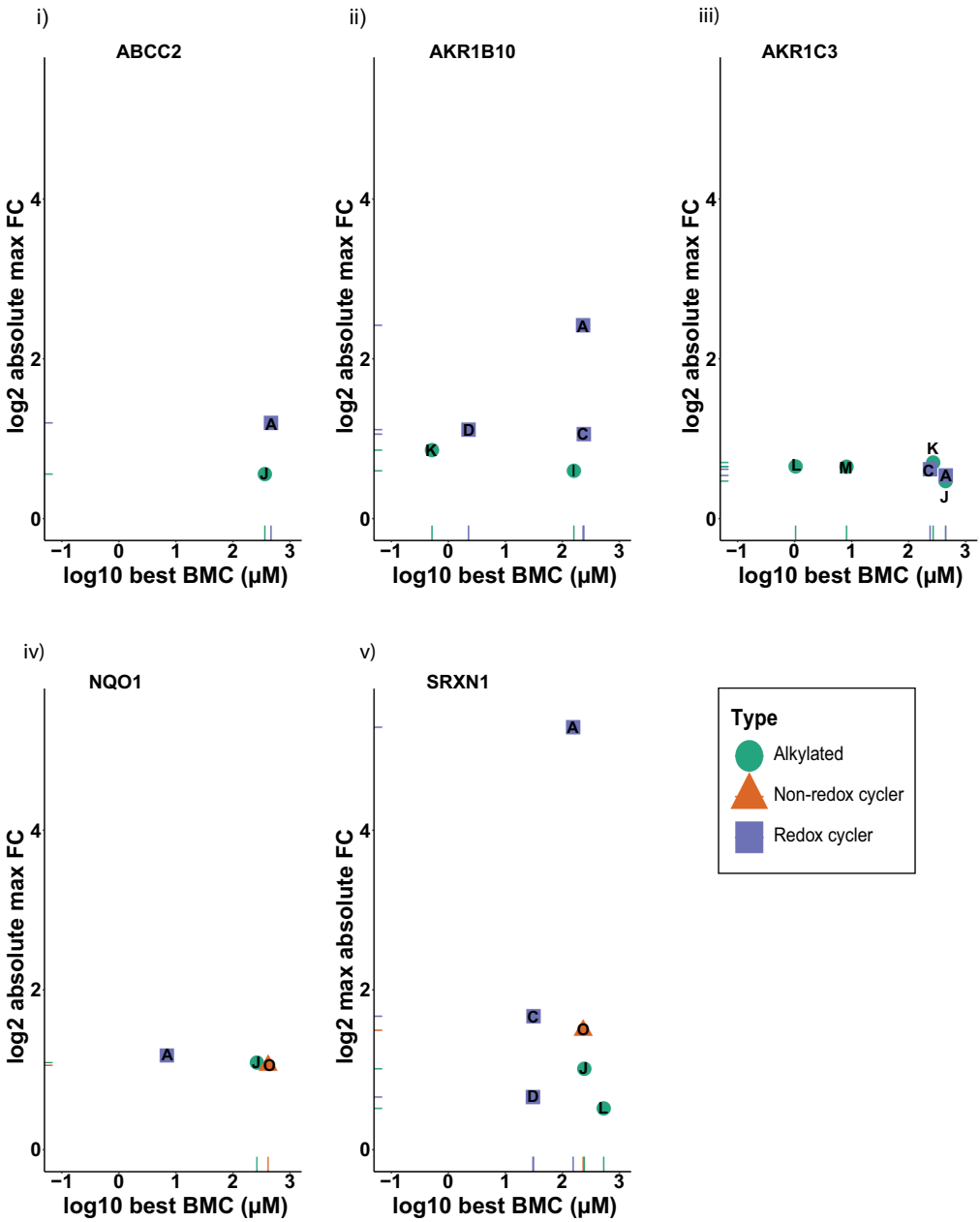

best BMC (benchmark concentration) (log10µM) of the Nrf2 target genes in Bi. **C)** Scatterplots of best log10 BMC vs log2 max absolute FC for the five selected Nrf2 target genes for the three different classes of phenolic compounds; only compounds with quantifiable values are depicted. A = Catechol, B = Trimethylbenzene-1,4-diol, C = tert-Butylhydroquinone, D = Hydroquinone, E = TMPPD, F = 2-Methyl-1,4-naphthoquinone, G = 2,4-Dimethylphenol, H = 2-(1,1-Dimethylethyl)phenol, I = p-tert-Butylphenol, J = 4-Methylphenol, K = 2,3,6-Trimethylphenol, L = 2,3,5-Trimethylphenol, M = 2,6-Dimethylphenol, N = 2,6-Di-tert-butyl-4-ethylphenol, O = Phenol, P = Resorcinol.

the PHH regarding the assessment of the effect of different phenolic compounds on the modulation of the Nrf2 pathway demonstrated that PHH had a smaller window of response due to increased sensitivity for the onset of cytotoxicity. Regardless of this increased sensitivity of PHH, we identified Srxn1 as the most optimal marker that can inform on activation of the Nrf2 pathway in both HepG2 and PHH.

A)

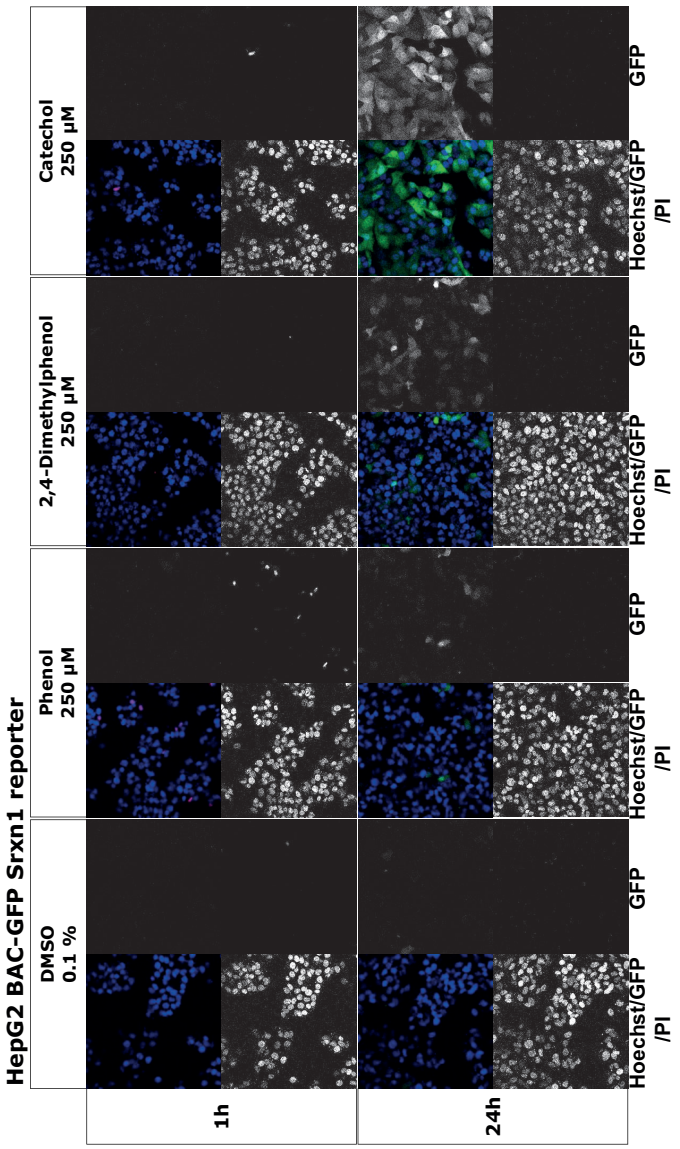

Figure 5. Effect of different phenolic compounds on Nrf2 activation and Srxn1 induction in HepG2 GFP reporter cell lines.

A) Effect of various phenolic compounds on GFP-Srxn1 induction in the HepG2 GFP-Srxn1 reporter cell line based on confocal microscopy at 1 and 24 hour after treatment. Each subpanel contains a composite image (upper left), Hoechst33342 picture (lower left), GFP picture (upper right) and propidium iodide (lower right). All images have same brightness/contrast settings. Note that no cell death was observed up till 24 hour treatment. Scale bar = 50 µm. **B)** Time response curves of Srxn1-GFP activation and Nrf2-GFP translocation to the nucleus after exposure to 250 µM of different phenolic compounds.

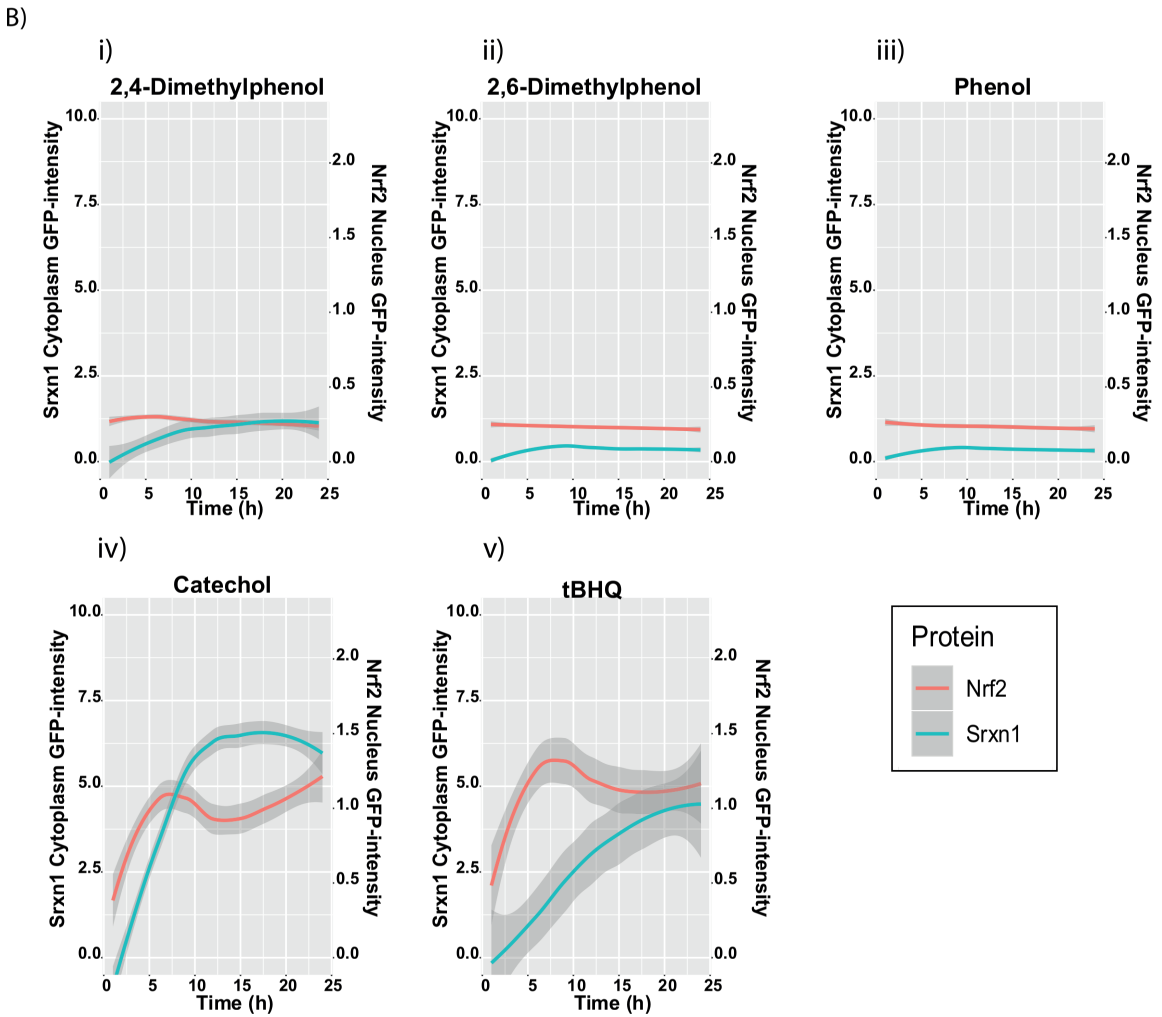

Srxn1 as biomarker to discriminate different phenolic compounds

The transcriptomics data above indicate that Srxn1 is the most optimal sensitive biomarker to determine Nrf2 pathway activation in both HepG2 and PHH. Next we aimed to translate transcriptomics information to protein level and relate this to Nrf2 activity. We previously established HepG2-GFP-reporter cell lines for Nrf2 and its downstream target Srxn1 (Wink et al. 2017) that allow the high throughput imaging-based quantitative assessment of Nrf2 stabilization and nuclear translocation and Srxn1 activation. These reporters are strongly activated by prototypical Keap1 modulators (Wink et al. 2017). Reporter cells were exposed to all the phenolic compounds that were used for transcriptomics in HepG2 and PHH, and we further expanded the number of alkylated phenols. Then Nrf2-GFP translocation to the nucleus and cytoplasmic Srxn1-GFP induction was measured every hour for 24 hours using quantitative live cell confocal microscopy (Figure 5A; see Figure 1D for all phenolic compounds). We observed clear dose response early activation of Nrf2-GFP followed by a later induction of Srxn1-GFP for the redox cycling phenols catechol and tBHQ (Figure 5B). The alkylated phenols such as 2,6-dimethylphenol and non-redox cycling phenols did not show a response. Yet, 2,4-dimethylphenol caused a mild induction Srxn1-GFP expression, which was corresponding to the Srxn1 mRNA expression observed with the transcriptomics analysis in the parental HepG2 cells. Next, for all the phenolic compounds tested we determined the maximal absolute log2 FC for the entire concentration time course data as well as the best log10 BMC. Redox cycling phenols showed the best absolute log2 FC accompanied with a lower best log10 BMC for both Nrf2-GFP activation and Srxn1-GFP induction (Figure 6A; and see Suppl. Table 2 for summary). None of the alkylating phenols was a strong activator of the Nrf2 pathway reporters. We explored further if we could integrate the FC and BMC information from our transcriptomics and GFP reporter assays. When comparing the expression changes (best absolute log2 FC) of Srxn1 protein expression to *SRXN1* gene expression changes, we observed a clear separation of the redox cyclers and alkylating phenols (Figure 6B). Similarly, the same pattern was found when comparing Srxn1-GFP log10 best BMC to the *SRXN1* gene log10 best BMC (Figure 6B).

DISCUSSION

Here we systematically determined a testing strategy for assessment of Nrf2 pathway activation for application in a read across approach. The present study describes the application of a high throughput transcriptomics analysis in HepG2 and PHH in combination with high throughput single cell imaging of GFP-Srxn1 reporter system. As a proof of concept, we aimed to identify whether certain classes

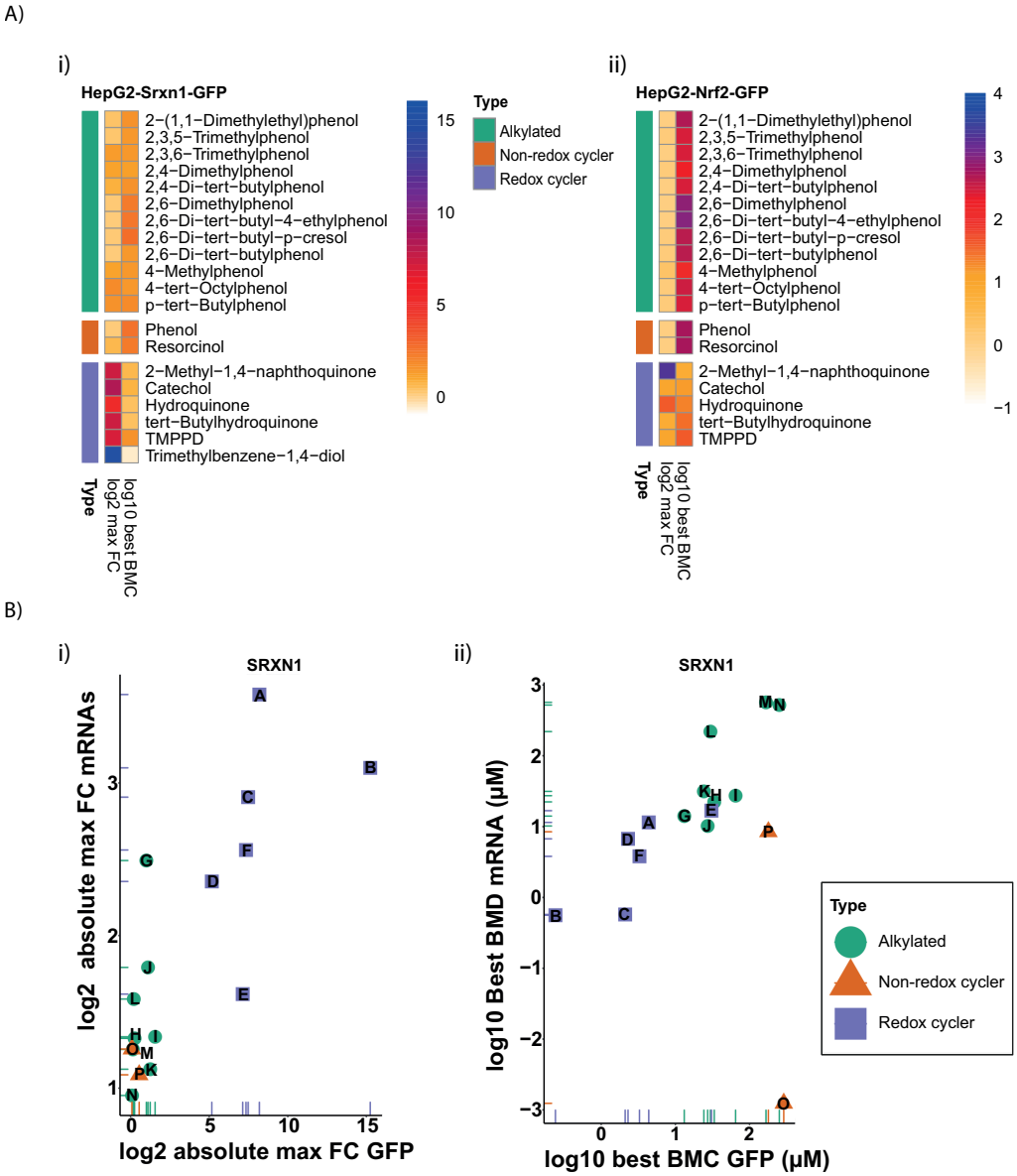

Figure 6. Effect of Nrf2 and Srxn1 response in HepG2 fluorescent protein reporter cells after phenolic compound exposure and relation with gene expression.

A) Heatmap of **i)** Srxn1-GFP response (max log2 FC and log10 best BMC (µM)) and **ii)** Nrf2-GFP response (max log2 FC and log10 best BMC) after exposure to different concentrations of phenolic compounds to HepG2 cells after 24h exposure. **B)** Scatterplot of: **i)** max absolute log2 FC-Srxn1-GFP versus max absolute log2 FC-SRXN1 gene expression and **ii)** log10 best BMC-Srxn1-GFP versus log10 best BMC-Srxn1 gene expression after 24h exposure of different classes of phenolic compounds. A = Catechol, B = Trimethylbenzene-1,4-diol, C = tert-Butylhydroquinone, D = Hydroquinone, E = TMPPD, F = 2-Methyl-1,4-naphthoquinone, G = 2,4-Dimethylphenol, H = 2-(1,1-Dimethylethyl)phenol, I = p-tert-Butylphenol, J = 4-Methylphenol, K = 2,3,6-Trimethylphenol, L = 2,3,5-Trimethylphenol, M = 2,6-Dimethylphenol, N = 2,6-Di-tert-butyl-4-ethylphenol, O = Phenol, P = Resorcinol.

of phenolic compounds (redox cyclers, non-redox cyclers, and alkylated phenols) can be classified based on their potential to induce the oxidative stress response. Based on exposure to different compounds which are known to induce the Nrf2-pathway, we identified the five most responsive genes out of a set of 36 Nrf2 related genes: *ABCC2*, *AKR1B10*, *AKR1C3*, *NQO1*, and *SRXN1*. The same genes also stood out for most phenolic redox cyclers.

Comparison of the Nrf2 target genes responses between HepG2 and PHH demonstrated that *SRXN1* showed the strongest resemblance in response. *SRXN1* plays a critical role in counteracting ROS (Findlay et al. 2006; Jeong et al. 2006; Ross and Siegel 2017; Siegel et al. 2018). We have previously reported on the dependence of Srxn1 expression on Nrf2 activation (Wink et al. 2017). The induction of Srxn1 gene expression by both our training pro-oxidants as well as the redox cycling phenols was highly sensitive. This sensitivity was also reflected by the GFP-Srxn1 induction in the reporter cell line. The latter reporter responses also allowed single cell time-resolved analysis of Nrf2 activation to also define similarity in temporal responses, thereby providing further support for biological similarity for read across.

AKR1B10 and *AKR1C3* were two genes found in the top 5 of most response Nrf2 targets and are members of the superfamily of the aldo-keto reductases (AKRs). AKRs can reduce carbonyl substrates, including quinones (Penning 2015), and play an important role in the detoxification of chemicals. Our previous studies using siKEAP1 and siNFE2L2 indicated the dependence on Nrf2 pathway activation for the induction of both AKR1B10 and AKR1C3 (Copple et al. 2019). *AKR1B10* was much more sensitive for induction by our pro-oxidants and followed a similar pattern as *SRXN1*. *AKR1C3* and *AKR1B10* are expressed at higher levels in HepG2 cells compared to other cell lines (Ebert et al. 2011) and therefore might be picked up easily in our studies. This may be related to the fact that *AKR1B10* is overexpressed in early stages of hepatocellular carcinoma (HCC), but down regulated in advanced tumor stages (Heringlake et al. 2010). Interestingly, also *AKR1C3* plays a role in the cytoprotection and is involved in the detoxification of ROS in association with resistance to radiotherapy in esophageal carcinoma cells (Xiong et al. 2014). Since *AKR1B10* induction was very strong in both HepG2 and PHH and activated by various pro-oxidants, we propose that *AKR1B10* could be an additional relevant sensitive reporter for Nrf2 pathway activation and, thereby, contributing to weight-of-evidence in read across when used in combination with the GFP-Srxn1 reporter.

We observed higher sensitivity in HepG2 cells to distinguish redox cyclers and non-redox cyclers/alkylated phenolic compounds than PHH. This might be due to a higher

biotransformation capacity of PHH, and therefore the ability of converting alkylated/non-redox cyclers into redox cyclers like quinone species. HepG2 cells are known for the inferior phase I and II biotransformation enzyme expression levels, that can impair their ability to successfully metabolize alkylated/non-redox cyclers (Jennen et al. 2010). However, it is also known that PHH lose their metabolic capacity rapidly in culture and therefore lose their close resemblance to the physiological situation in humans. Of relevance is that PHH were more sensitive towards redox cycling induced cell death, which might indicate a high hepatic vulnerability towards oxidative stress induced by redox cycling phenolic compounds. This was successfully substantiated in the HepG2 reporter with the ability to detect this redox-cycling activity as mode of action.

Although most alkylated phenolic compounds showed no or only a minor response in activating Nrf2 related genes, 2,4-dimethylphenol was found as one of the most active alkylated phenolic compounds in HepG2 cells as assessed by transcriptomic analysis. A similar observation was made in PHH. Interestingly 2,6-dimethylphenol gave a far lower response indicating that minor differences in the phenols can have major impact on biological effects. Hence, care should be taken with sole evaluation of read across on structural similarity, but also involve a systematic evaluation of similarity of biological effects including potency evaluation such as using transcriptomic analysis.

Recently we have evaluated the experimental requirements to study phenols in relation to volatility (Tolosa et al. 2021). Based on these studies, here we used membranes to prevent loss of volatile phenolic compounds. We cannot exclude that we have lost some parent compounds in our HepG2 and PHH test systems during the 24 h exposure through other routes, including metabolism or degradation. Given that the phenols have a direct effect on Nrf2-GFP activation within the first 8 hours as well as the direct subsequent induction of Srxn1-GFP, we anticipate that we can faithfully determine differences in the proximal mode-of-action of the entire panel of phenols used in this study. This underscores the applicability of these reporter systems, since we can monitor the temporal response of the Nrf2 pathway activation at the individual cell level over time, including early time points. The transcriptomics responses were determined 24 hour after treatment and largely correlated with the anticipated effects of redox-cycling and alkylated phenols, in particular in HepG2 cells. However, we cannot exclude that some of the transcriptomics responses at the late 24 h time point are partially related to metabolites derived from the parent phenols.

In summary, we demonstrate that integration of high throughput HepG2 Nrf2 pathway reporter cell line data in combination with transcriptomics data from HepG2 and PHH, provides valuable mechanistic information on mode-of-action of structural similar phenols and their biological similarity. We anticipate that integration of these strategies, in combination with further information on toxicokinetics of these compounds, will provide a valuable approach for a read across assessment. Therefore, we foresee the use of this new approach methodology as a major part of an integrated approach for chemical safety testing with respect to a compounds potential to induce oxidative stress.

ACKNOWLEDGMENTS

This work was supported by the Ministry of Defence of the Netherlands and the European Commission Horizon2020 EU-ToxRisk project (grant nr 681002).

REFERENCES

Attia SM (2010) Deleterious effects of reactive metabolites. Oxid Med Cell Longev 3(4):238-53 doi:10.4161/oxim.3.4.13246

Benfenati E, Chaudhry Q, Gini G, Dorne JL (2019) Integrating in silico models and read-across methods for predicting toxicity of chemicals: A step-wise strategy. Environ Int 131:105060 doi:10.1016/j.envint.2019.105060

Bischoff LJM, Kuijper IA, Schimming JP, et al. (2019) A systematic analysis of Nrf2 pathway activation dynamics during repeated xenobiotic exposure. Arch Toxicol 93(2):435-451 doi:10.1007/s00204-018-2353-2

Biteau B, Labarre J, Toledano MB (2003) ATP-dependent reduction of cysteine–sulphinic acid by S. cerevisiae sulphiredoxin. Nature 425(6961):980-984 doi:10.1038/nature02075

Bolton JL, Dunlap T (2017) Formation and Biological Targets of Quinones: Cytotoxic versus Cytoprotective Effects. Chem Res Toxicol 30(1):13-37 doi:10.1021/acs.chemrestox.6b00256

Bolton JL, Trush MA, Penning TM, Dryhurst G, Monks TJ (2000) Role of Quinones in Toxicology. Chemical Research in Toxicology 13(3):135-160 doi:10.1021/tx9902082

Bushel PR, Paules RS, Auerbach SS (2018) A Comparison of the TempO-Seq S1500+ Platform to RNA-Seq and Microarray Using Rat Liver Mode of Action Samples. Front Genet 9:485-485 doi:10.3389/fgene.2018.00485

Copple IM, den Hollander W, Callegaro G, et al. (2019) Characterisation of the NRF2 transcriptional network and its response to chemical insult in primary human hepatocytes: implications for prediction of drug-induced liver injury. Arch Toxicol 93(2):385-399 doi:10.1007/s00204-018-2354-1

Daneshian M, Kamp H, Hengstler J, Leist M, van de Water B (2016) Highlight report: Launch of a large integrated European in vitro toxicology project: EU-ToxRisk. Archives of toxicology 90(5):1021-1024 doi:10.1007/s00204-016-1698-7

Ebert B, Kisiela M, Wsol V, Maser E (2011) Proteasome inhibitors MG-132 and bortezomib induce AKR1C1, AKR1C3, AKR1B1, and AKR1B10 in human colon cancer cell lines SW-480 and HT-29. Chem Biol Interact 191(1-3):239-49 doi:10.1016/j.cbi.2010.12.026

ECHA (2016) New Approach Methodologies in Regulatory Science: Proceedings of a Scientific Workshop, April 2016. Available at: https://echa.europa.eu/documents/10162/21838212/scientific_ws_proceedings_en.pdf/a2087434-0407-4705-9057-95d9c2c2cc57. In.

Escher SE, Kamp H, Bennekou SH, et al. (2019) Towards grouping concepts based on new approach methodologies in chemical hazard assessment: the read-across approach of the EU-ToxRisk project. Arch Toxicol 93(12):3643-3667 doi:10.1007/s00204-019-02591-7

Findlay VJ, Townsend DM, Morris TE, Fraser JP, He L, Tew KD (2006) A novel role for human sulfiredoxin in the reversal of glutathionylation. Cancer Res 66(13):6800-6 doi:10.1158/0008-5472.CAN-06-0484

Graepel R, Ter Braak B, Escher SE, et al. (2019) Paradigm shift in safety assessment using new approach methods: The EU-ToxRisk strategy. Current Opinion in Toxicology 15:33-39 doi:10.1016/j.cotox.2019.03.005

Heringlake S, Hofdmann M, Fiebeler A, Manns MP, Schmiegel W, Tannapfel A (2010) Identification and expression analysis of the aldo–ketoreductase1-B10 gene in primary malignant liver tumours. Journal of Hepatology 52(2):220-227 doi:https://doi.org/10.1016/j.jhep.2009.11.005

Jennen DG, Magkoufopoulou C, Ketelslegers HB, van Herwijnen MH, Kleinjans JC, van Delft JH (2010) Comparison of HepG2 and HepaRG by whole-genome gene expression analysis for the purpose of chemical hazard identification. Toxicol Sci 115(1):66-79 doi:10.1093/toxsci/kfq026

Jeong W, Park SJ, Chang TS, Lee DY, Rhee SG (2006) Molecular mechanism of the reduction of cysteine sulfinic acid of peroxiredoxin to cysteine by mammalian sulfiredoxin. J Biol Chem 281(20):14400-7 doi:10.1074/jbc.M511082200

Keum YS, Choi BY (2014) Molecular and chemical regulation of the Keap1-Nrf2 signaling pathway. Molecules 19(7):10074-89 doi:10.3390/molecules190710074

Kobayashi A, Kang MI, Okawa H, et al. (2004) Oxidative stress sensor Keap1 functions as an adaptor for Cul3-based E3 ligase to regulate proteasomal degradation of Nrf2. Mol Cell Biol 24(16):7130-9 doi:10.1128/MCB.24.16.7130-7139.2004

Kyselova Z (2011) Toxicological aspects of the use of phenolic compounds in disease prevention. Interdiscip Toxicol 4(4):173-83 doi:10.2478/v10102-011-0027-5

Love MI, Huber W, Anders S (2014) Moderated estimation of fold change and dispersion for RNA-seq data with DESeq2. Genome Biol 15(12):550-550 doi:10.1186/s13059-014-0550-8

Mav D, Shah RR, Howard BE, et al. (2018) A hybrid gene selection approach to create the S1500+ targeted gene sets for use in high-throughput transcriptomics. PLoS One 13(2):e0191105 doi:10.1371/journal.pone.0191105

Monks TJ, Hanzlik RP, Cohen GM, Ross D, Graham DG (1992) Quinone chemistry and toxicity. Toxicology and Applied Pharmacology 112(1):2-16 doi:https://doi.org/10.1016/0041-008X(92)90273-U

Monks TJ, Lau SS (1997) Biological reactivity of polyphenolic-glutathione conjugates. Chem Res Toxicol 10(12):1296-313 doi:10.1021/tx9700937

Parish ST, Aschner M, Casey W, et al. (2020) An evaluation framework for new approach methodologies (NAMs) for human health safety assessment. Regul Toxicol Pharmacol 112:104592 doi:10.1016/j.yrtph.2020.104592

Penning TM (2015) The aldo-keto reductases (AKRs): Overview. Chem Biol Interact 234:236-46 doi:10.1016/j.cbi.2014.09.024

Perkins EJ, Ashauer R, Burgoon L, et al. (2019) Building and Applying Quantitative Adverse Outcome Pathway Models for Chemical Hazard and Risk Assessment. Environ Toxicol Chem 38(9):1850-1865 doi:10.1002/etc.4505

Phillips JR, Svoboda DL, Tandon A, et al. (2018) BMDExpress 2: enhanced transcriptomic dose-response analysis workflow. Bioinformatics 35(10):1780-1782 doi:10.1093/bioinformatics/bty878

Priya S, Nigam A, Bajpai P, Kumar S (2014) Diethyl maleate inhibits MCA+TPA transformed cell growth via modulation of GSH, MAPK, and cancer pathways. Chem Biol Interact 219:37-47 doi:10.1016/j.cbi.2014.04.018

Ross D, Siegel D (2017) Functions of NQO1 in Cellular Protection and CoQ10 Metabolism and its Potential Role as a Redox Sensitive Molecular Switch. Front Physiol 8:595 doi:10.3389/fphys.2017.00595

Schimming JP, ter Braak B, Niemeijer M, Wink S, van de Water B (2019) System Microscopy of Stress Response Pathways in Cholestasis Research. In: Vinken M (ed) Experimental Cholestasis Research. Springer New York, New York, NY, p 187-202

Siegel D, Dehn DD, Bokatzian SS, et al. (2018) Redox modulation of NQO1. PLoS One 13(1):e0190717 doi:10.1371/journal.pone.0190717

Takaya K, Suzuki T, Motohashi H, et al. (2012) Validation of the multiple sensor mechanism of the Keap1-Nrf2 system. Free Radic Biol Med 53(4):817-27 doi:10.1016/j.freeradbiomed.2012.06.023

Tolosa L, Martínez-Sena T, Schimming JP, et al. (2021) The in vitro assessment of the toxicity of volatile, oxidisable, redox-cycling compounds: phenols as an example. Archives of toxicology 95(6):2109-2121 doi:10.1007/s00204-021-03036-w

Wambaugh JF, Bare JC, Carignan CC, et al. (2019) New approach methodologies for exposure science. Current Opinion in Toxicology 15:76-92 doi:10.1016/j.cotox.2019.07.001

Wink S, Hiemstra S, Herpers B, van de Water B (2017) High-content imaging-based BAC-GFP toxicity pathway reporters to assess chemical adversity liabilities. Arch Toxicol 91(3):1367-1383 doi:10.1007/s00204-016-1781-0

Wink S, Hiemstra SW, Huppelschoten S, Klip JE, van de Water B (2018) Dynamic imaging of adaptive stress response pathway activation for prediction of drug induced liver injury. Arch Toxicol doi:10.1007/s00204-018-2178-z

Xiong R, Siegel D, Ross D (2014) Quinone-induced protein handling changes: implications for major protein handling systems in quinone-mediated toxicity. Toxicol Appl Pharmacol 280(2):285-95 doi:10.1016/j.taap.2014.08.014

Yeakley JM, Shepard PJ, Goyena DE, VanSteenhouse HC, McComb JD, Seligmann BE (2017) A trichostatin A expression signature identified by TempO-Seq targeted whole transcriptome profiling. PLoS One 12(5):e0178302 doi:10.1371/journal.pone.0178302

Zipper LM, Mulcahy RT (2002) The Keap1 BTB/POZ dimerization function is required to sequester Nrf2 in cytoplasm. J Biol Chem 277(39):36544-52 doi:10.1074/jbc.M206530200

SUPPLEMENTAL MATERIALS

Supplemental Table 1: Gene list overlap between Nrf2 regulated genes EU-ToxRisk S1500+ V2 TempO-Seq gene panel (= 36 Nrf2 related genes).

Gene symbol	Ensembl ID	Gene symbol	Ensembl ID
ABCB6	ENSG00000115657	MAP2	ENSG00000078018
ABCC2	ENSG00000023839	MAPT	ENSG00000186868
ABHD4	ENSG00000100439	MLLT11	ENSG00000213190
AFP	ENSG00000081051	NQO1	ENSG00000181019
AKR1B10	ENSG00000198074	OSGIN1	ENSG00000140961
AKR1C3	ENSG00000196139	PPARA	ENSG00000186951
ALDH3A2	ENSG00000072210	PRDX1	ENSG00000117450
CBR1	ENSG00000159228	SCCPDH	ENSG00000143653
CBR3	ENSG00000159231	SFN	ENSG00000175793
CCND1	ENSG00000110092	SLCO1B1	ENSG00000134538
CES1	ENSG00000198848	SOD1	ENSG00000142168
EPHX1	ENSG00000143819	SPP1	ENSG00000118785
GPX2	ENSG00000176153	SRXN1	ENSG00000271303
GSR	ENSG00000104687	SULT1A2	ENSG00000197165
GSTA4	ENSG00000170899	TXNRD1	ENSG00000198431
GSTA5	ENSG00000182793	UGDH	ENSG00000109814
IKBKG	ENSG00000269335	UGT1A6	ENSG00000167165
MAFG	ENSG00000197063	UGT1A8	ENSG00000242366

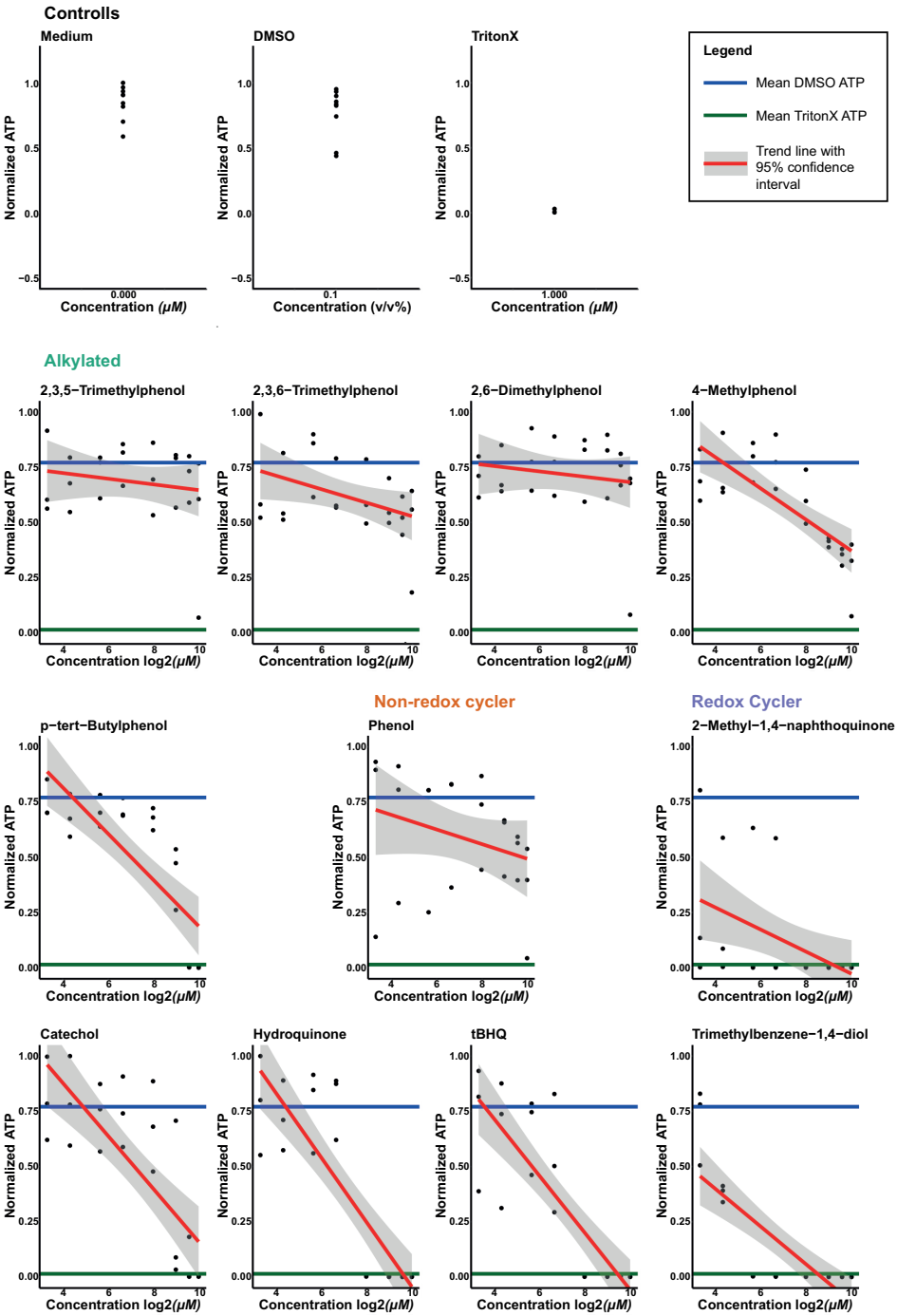

Supplemental Figure 1. Effect of phenolic compounds on PHH viability.

Viability was determined by ATP content of PHH. Three measurements per concentration are shown and six for the controls. ATP levels were measured 24 h after exposure.

Supplemental Table 2. Effect of Nrf2 and Srxn1 response in HepG2 fluorescent protein reporter cells after phenolic compound exposure and relation with gene expression.

Srxn1-GFP response (max log2 FC and log10 best BMC (μM)) and Nrf2-GFP response (max log2 FC and log10 best BMC (μM)) after exposure to different concentrations of phenolic compounds to HepG2 cells after 24 h exposure.

		SRXN1		NRF2	
Compound	**Type**	**log2_FC**	**log10_BMC**	**log2_FC**	**log10_BMC**
2-(1,1-Dimethylethyl)phenol	Alkylated	0.254064686	1.524681663	0.0477701	2.688186593
2,3,5-Trimethylphenol	Alkylated	0.203229098	1.473098486	0.1017354	2.454340176
2,3,6-Trimethylphenol	Alkylated	1.250000243	1.38433549	0.0348152	2.421794711
2,4-Dimethylphenol	Alkylated	1.002061115	1.120096603	0.101833	2.280921937
2,4-Di-tert-butylphenol	Alkylated	0.692341787	1.582353175	0.0348152	2.421794711
2,6-Dimethylphenol	Alkylated	0.144863275	2.22224291	0.0303122	2.91131105
2,6-Di-tert-butyl-4-ethylphenol	Alkylated	0.09451427	2.401963724	0.0279593	2.958588249
2,6-Di-tert-butyl-p-cresol	Alkylated	0.159260826	2.594364923	0.066368	2.599238791
2,6-Di-tert-butylphenol	Alkylated	0.102174362	1.380393969	0.066368	2.599238791
4-Methylphenol	Alkylated	1.10856306	1.435627802	0.2853099	2.166684636
4-tert-Octylphenol	Alkylated	1.763377625	1.364596017	0.0686018	2.466499871
p-tert-Butylphenol	Alkylated	1.559155564	1.812247373	0.0980131	2.411845211
Phenol	Non redox cycler	0.08445872	2.461722069	0.0345162	2.754764081
Resorcinol	Non redox cycler	0.546179954	2.254463482	0.0347753	2.743064267
2-Methyl-1,4-naphthoquinone	Redox cycler	7.343117656	0.516101524	3.2964561	0.868288159
Catechol	Redox cycler	8.192966392	0.640883743	0.9853045	1.143102275
Hydroquinone	Redox cycler	5.167800943	0.361644746	1.60402	1.324950878
tert-Butylhydroquinone	Redox cycler	7.479745856	0.323076696	0.829921	1.462285666
TMPPD	Redox cycler	7.133384638	1.486129982	0.9502092	1.599766299
Trimethylbenzene-1,4-diol	Redox cycler	15.24768824	-0.617410283	NA	NA